euronoise

Local patch acoustic holography methods in enclosed spaces

Zdenek Havranek and Ludvik Bejcek

Brno University of Technology, UAMT-FEEC, Kolejni 4, 61200 Brno, Czech Republic
havranek@feec.vutbr.cz

The paper compares reconstruction accuracy and computational cost of three patch acoustic holography algorithms applicable in the enclosed spaces for prediction of sound field near sources. Algorithms under investigation were DL-SONAH, classical NAH with spatial transformations and hologram aperture enlargement and IBEM. All of the selected algorithms take an advantage of using double layer microphone array for measurement of sound pressure field. The reconstruction accuracy of all algorithms is determined by using of simple 3D model of curved radiating surface on the basis of calculation of difference between true acoustic quantity (pressure, velocity or intensity) values very close to the surface and predicted sound field at same positions. All these methods use different calculation procedure to obtain predicted sound field near source surface, thus comparison of effectiveness of these algorithms including prediction accuracy-to-computational cost ratio is useful to determination their applicability in practice. Results of prediction error and calculation time are presented and compared.

1 Introduction

Analyses of vibrations of real structures are usually needed in technical diagnostics. Localization of sound sources and finding the position of impacting force which causes the vibrations of the structure is a difficult task, especially when this information is required quickly and has to be realistic, thus without any influence of measuring device upon the measured object.

The procedure for localization of sound sources and their characterization in near-field called acoustic holography (NAH) was presented in ‘80s by Williams and Maynard. The basic theory for planar holography was transformed to polar and cylindrical coordinates and uses not only plane wave decomposition. Also other methods, which overcome problems with discrete Fourier transformation, have been presented in the past.

For accurate sound field reconstruction, the most of the derivations assume that sound sources are only on the one side of the measurement plane. If there is another source behind, background noise or reflections from the rear wall, many of the algorithms fail.

One recent derivation developed by Hald in ‘90s and published later with acronym SONAH (Statistically Optimized NAH) predicts sound field near source surface directly in spatial domain without transformation to wavenumber domain [1,2]. This approach allows prediction of sound field with smaller microphone array than sound source and utilizes data from all microphone positions while classical near-field acoustic holography (NAH) based on spatial transformation destroys measured data on edges of microphone array by spatial windowing. These “full field” methods are usually called patch holography methods. The methods based on spatial transformations are usually faster than patch holography methods due to easy implementation of 2D-FFT, but some present implementations of patch methods are also very fast and allow real time data processing [4,5,6]. Other calculation procedures for determination of the positions of the sound sources and their characterization based on boundary and finite element methods has been described and evaluated in the last decade [10].

All these methods (limited or full field) are only used for estimation of position of sound source and rough characterization of the source strength, due to many reasons. The knowledge of the source geometry is one of the most important parameter, but it is not known in most cases (geometry is not simply planar) and causes huge prediction error of the acoustical quantities near source surface and getting localization more difficult. In that cases where 3D model of the object geometry is known or can be entered as an input parameter for calculation (boundary element model or finite element model) more accurate characterization of sound sources can be achieved. Another parameter which affects the prediction accuracy is free field condition of measurement of acoustical quantities obtained by the array. This means source free region in front of the examined vibrating surface and no reflection from other objects. In real world conditions this prerequisite is hardly fulfilled and thus the localization is complicated and inaccurate in enclosed areas.

Determination of source strength and localization of the sources of vibrations induced by mechanical forces is important in technical diagnostics of machinery for estimation of expected remaining operating hours or prediction of the fail. Also in the procedure of the design of new machines or devices where the amount of acoustic pollution is reduced (passenger cars, public transport vehicles, airplanes, etc.) the knowledge of the sources of noise and vibrations is very important for improvement of acoustical comfort and reduction of overall emission of the unwanted vibrations. Many ongoing EU projects are trying to improve the design of the cars, aircraft, trains, etc. with respect to their noise and vibration pollution.

2 Short overview of the theory

In this investigation, the main interest has been focused on algorithms for patch near-field holography (NAH) calculation using double layer array as a field pressure measurement device. Patch NAH algorithms allow the prediction of sound field near sources where source surface size is larger than microphone array. The algorithms under investigation are taking advantage of using double layer microphone array (DLA) where there is a possibility for extraction of inward and outward sound field (ability to distinguishing between sources in front of the DLA and behind it). Three different NAH algorithms have been selected for testing and comparison through simulated measurements. All algorithms involves different calculation procedure, thus their comparison could give an overview of the qualities, weaknesses and determination their applicability in practice.

2.1 Double Layer SONAH

As the first representative of the patch methods, the algorithm without spatial transformations has been chosen.

The Double Layer SONAH (DL-SONAH) predicts sound field near sources on assumption that certain set of elementary waves, where one can be defined by Eq.(1), can describe total sound field produced by one examined source additionally with other non-zero disturbing sources.

$$\Phi_{\mathbf{K}}(x,y,z) = e^{j(k_x x + k_y y + k_z z)} \quad (1)$$

This idea can be expressed by Eq.(2) and the corresponding pressure field will use same set of coefficients c_n, which represent the original amplitude of each elementary wave at source position.

$$\Phi_{\mathbf{K}_m}(x,y,z) \approx \sum_{n=1}^{N} c_n(x,y,z_x)\Phi_{\mathbf{K}_m}(x_n,y_n,z) \quad (2)$$

The pressure field in prediction plane calculated from measured field pressures can be described by Eq.(3).

$$p(x,y,z_x) \approx \sum_{n=1}^{N} c_n(x,y,z_x)p(x_n,y_n,z_\mathrm{h}) \quad (3)$$

The resulting pressure prediction calculation in matrix form for single layer calculation is simplified by Eq.(4).

$$\mathbf{p}_{zx} = \mathbf{p}_{zh}^{\mathrm{T}}(\mathbf{A}^{\mathrm{H}}\mathbf{A} + \theta^2\mathbf{I})^{-1}\mathbf{A}^{\mathrm{H}}\mathbf{b} \quad (4)$$

More detailed derivation can be found in [1] and expansion to double layer calculation, which can determine the direction of the waves (inward-outward; induced by the source or background noise), can be found in [2, 3].

2.2 NAH with spatial transformation

The second method under investigation uses classical NAH calculation with spatial transformation (ST-NAH) and with enlarging the hologram aperture and spatial filtering to reduce edge effects on the prediction surface. This method is not exactly "patch" method, but with used improvements (described later) can compete with above described true patch methods. The complication with prediction of small part of sound field near sound source surface much larger than array with strong energy far from the array can still arise, but its influence will be reduced.

The original method without enlarging hologram aperture can't be used with patch-to-patch measurements due to huge reconstruction errors on the edges of the prediction plane caused by windowing in spatial domain. With the expansion of the hologram plane aperture, the damaged pressure information can be restored with iterative procedure involving low filtration of evanescent waves (in the k-space) in the band closed to the maximal spatial frequency of used microphone array. The iterative procedure can be written by Eq.(5).

$$p_{zh_{1,2}}^{n(4Mx4N)} = F_{x,y}^{-1}\left[F_{x,y}\left[p_{zh_{1,2}}^{n-1(4Mx4N)}\right]K_f\right] \leftarrow p_{zh_{1,2}}^{orig(MxN)} \quad (5)$$

In the first step, original hologram aperture is enlarged with zero padding. The next step involves direct and indirect spatial transformation while filtering in k-space is applied. The resulting pressure data in spatial domain is then corrected with true measured (original) pressure data. The procedure is finished when the difference between transformed spatial pressure data and original measured pressure data is minimal.

Restored pressure data in spatial domain can then be fully used into transformation to k-space, where the kernel of the double layer NAH calculation is applied. The basic kernel procedure for double layer processing in wavenumber domain is described by Eq.(6) and in more detail presented in [4, 5].

$$P_{zh}(k_\mathrm{x},k_y) = \frac{P_{zh1}(k_\mathrm{x},k_y) - P_{zh2}(k_\mathrm{x},k_y)e^{i\bar{k}_z D}\cdot K_f(k_\mathrm{x},k_y)}{\left(1-e^{i2\bar{k}_z D}\right)\cdot K_f(k_\mathrm{x},k_y)} \quad (6)$$

The Eq.(5) contains image of pressure measured in 1st plane (layer) $P_{zh1}(k_x, k_y)$ and image of pressure measured in 2nd plane (layer) $P_{zh2}(k_x, k_y)$, a distance between layers D and k-space filter (Harris cosine window) $K_f(k_x, k_y)$. The k-filter can be described with Eq.(7a, 7b).

$$K_f(k_x,k_y) = 1 - \frac{1}{2}e^{(|k|/k_c - 1)/\alpha} \quad \text{for } |k| < k_c \quad (7a)$$

$$K_f(k_x,k_y) = \frac{1}{2}e^{(1-|k|/k_c)/\alpha} \quad \text{for } |k| > k_c \quad (7b)$$

Application of Harris cosine window in k-space leads to minimize errors caused by the using of non-ideal transducers (with amplitude and phase mismatch). The filtration in k-space minimizes evanescent waves coming from another sound source behind the double layer microphone array. One can assume that the other source is much far away than the examined source, so the disturbing source affects mostly the propagating part of the wave spectra of the source of interest and the filtration does not corrupt the important part of the acoustic field at microphone positions.

The first estimation of the reconstructed field is based on the result from separation of incoming and outcoming sound fields based on Eq.(6) and made with simple setting of wavenumber filter, where the cut-off frequency is selected to one half of the maximum spatial frequency of measurement, equals to stepping in space domain (distance between microphones). This estimation is later used in second iterative technique based on recursive Wiener filtering [7], Eq.(8), using filter described by Eq.(9).

$$P_{zx} = P_{zx-1} + W\cdot\left(P_{zh} - G_p\cdot P_{zx-1}\right) \quad (8)$$

$$W(k_x,k_y,z_h - z_x) = \frac{G_p^*}{|G_p|^2 + 10^{-\frac{SNR}{10}}} \quad (9)$$

Due to the strong amplification of evanescent components, when the noise is presented in the measurement, certain type of regularization in iterative algorithm has to be done. The transfer function of Wiener filter is supplemented with regularization coefficient which can be represented in Signal-to-Noise Ratio (SNR), describing the expected difference between measured values and overall noise in the measurement path. In this algorithm, the selection of the SNR value can be experimental, based on measured data, or by some parameter choice method [8, 9]. In this investigation the SNR value was chosen experimentally to obtain the best prediction accuracy.

2.3 Inverse BEM

The last method used in this investigation is Inverse Boundary Element Method (IBEM) using discretization of source surface and surroundings around microphone array into boundary elements which represents the acoustic quantities (pressure, normal velocity) on the boundary. The presented implementation uses double layer microphone array to estimate field velocity at first layer to enhance the accuracy of the prediction in the field points near or on the examined source surface.

IBEM uses inverse boundary element calculation with the boundary surrounding the microphone array and a part of source surface under investigation, the general matrix formula, which expresses this inverse calculation is defined by Eq.(10).

$$v_n = -\frac{1}{j\omega\rho}\left[GQ^{-1}B\right]^{-1} p_f \qquad (10)$$

The prediction of the acoustic quantities (velocity) near source surface is divided into three steps. In the first step, only calculation of velocity on artificial source surface, defined as first microphone layer, is performed. In this part of the calculation, the boundary model covers only double layer microphone array and the calculation of field point velocities (at the first layer microphone array) is performed. This situation in 3D space shows Fig. 1.

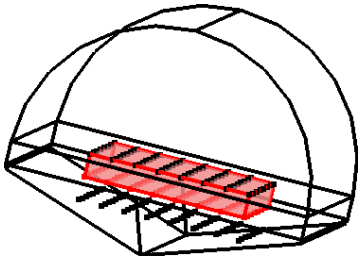

Fig.1 3D model of curved surface with highlighted first boundary element model area

The second step uses measured pressure and predicted velocity values on the front microphone layer to determine boundary values of the 3D boundary element model, Fig. 2.

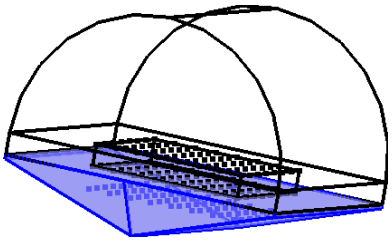

Fig.2 3D model of curved surface with highlighted second boundary element model area

The last step of the calculation is determination of normal velocities (normal to array plane) at defined field points (prediction points are blue color on Fig. 2) inside the second boundary element model. These values can be calculated directly by evaluating the Rayleigh integral.

The prediction accuracy can be enhanced with iterative technique on the first (front) microphone layer, where the knowledge of true measured pressure values can be used to correct velocity field data.

More details about general Inverse BEM can be found in [10].

3 Simulated experiments

3.1 Test case definition

Evaluation and comparison of algorithms in Matlab has been made on 3D model of curved surface designed in COMSOL with assigned sound source properties, definition of microphone position in 3D space and calculation points near source surface. The model parameters are space coordinates of field points and acoustic variables as sound pressure and normal velocity, or sound intensity, which is used as input data for all algorithms (pressure data at microphone positions in this case) and for comparison of results (sound field near source). The 3D model with field points of measured pressure and pressure field at microphone positions, when one part of the surface below the array acting as vibrating plate with defined velocity are shown on the Fig. 3.

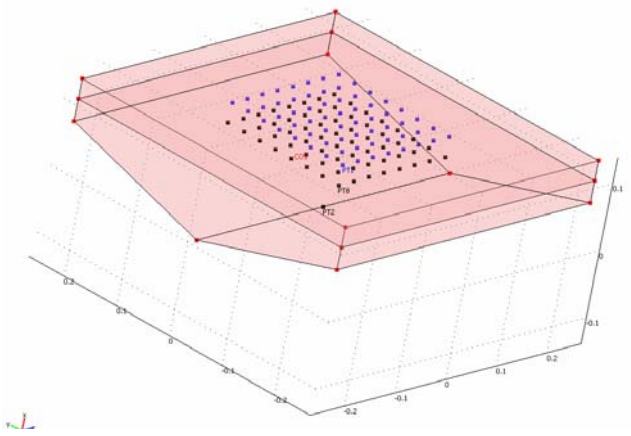

Fig.3 3D model of curved surface designed in COMSOL, free field conditions behind the array

For evaluation of the algorithms when the reflections are present, another 3D model has been used, Fig. 4. It incorporates background hard wall with defined acoustic impedance to reflect some part of incoming sound field produced by the source plate. This setup reflects more realistic measurement conditions in enclosed spaces.

The microphone array used in this setup has 8x8 microphones with 30 mm microphone spacing and 30 mm between layers. The prediction plane is 30 mm far from the front layer and the distance from the source surface vary from 5 mm to 40 mm.

The exact velocity field values at calculation points and field point pressures have been obtained by finite element simulation of 3D model with added artificial excitation of

one steel plate with thickness of 3 mm near the 3D corner below the array, Fig. 5. The exactly calculated velocity field values has been used as a reference for comparison and evaluation of the prediction accuracy of the algorithms.

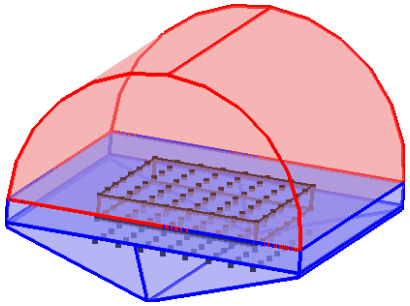

.Fig.4 3D model of curved surface designed in COMSOL, reflections from hard wall behind the array

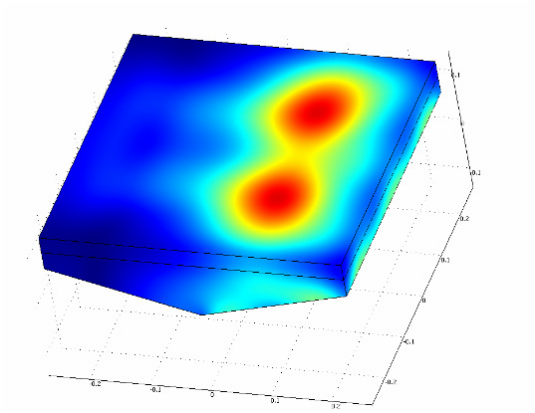

Fig.5 Pressure field distribution in 3D model for force excitation with frequency of 1000 Hz, background free field conditions

The error norm used for evaluation of the performance of the algorithms is the total mean square difference between the 'true' pressure and values calculated with each algorithm, normalized with the 'true' mean square values at all points in the examined positions. The error norm for the predicted velocity values at defined calculated points near source surface is defined by Eq.(11).

$$MSE = \sqrt{\frac{\sum_i \left| v_i^{true} - v_i \right|^2}{\sum_j \left| v_j^{true} \right|^2}} \cdot 100\% \qquad (11)$$

Due to simplification of the evaluation of the accuracy of the algorithms, the calculating points (where acoustic quantities are predicted) is selected in the plane very near curved surface. This is mainly required for NAH algorithm with spatial transformations where the prediction point should be in parallel plane to the measurement planes. There could the procedure to obtain predicted data in another parallel plane (closer to the corner of the vibrating plate), but it will cause additional computation which will probably increase the reconstruction error and the description of this treatment and its evaluation will extend this investigation unacceptably.

4 Results

4.1 Sound field prediction error

The comparison of results of the selected algorithms has been performed on the two described 3D models with evaluation of normal component of particle velocity predicted very close to the radiating surface (distance vary from 5 mm to 40 mm). The prediction accuracy has been computed in the frequency range of used microphone array and results for DL-SONAH are on Fig. 6.

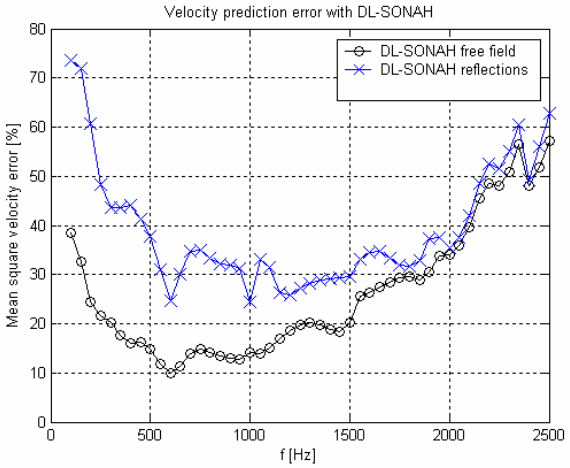

Fig.6 Comparison of normal velocity prediction error with DL-SONAH for two 3D models

The reconstruction accuracy for ST-NAH algorithm for two simulation cases is on the figure 7. In this case, the error norm is calculated only for field points inside the prediction grid, not on the edges, due to strong non-removable errors. This is one significant limitation of the proposed enhanced ST-NAH algorithm.

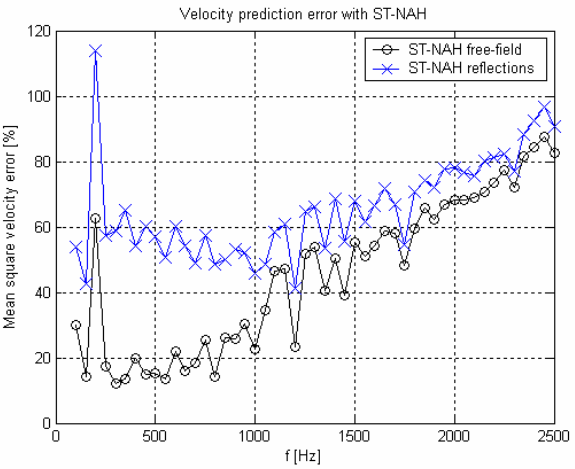

Fig.7 Comparison of normal velocity prediction error with ST-NAH for two 3D models (errors without boundary)

The last figure, Fig. 8, evaluates the accuracy of the true double layer IBEM algorithm on 3D model where reflections from behind of the array are present.

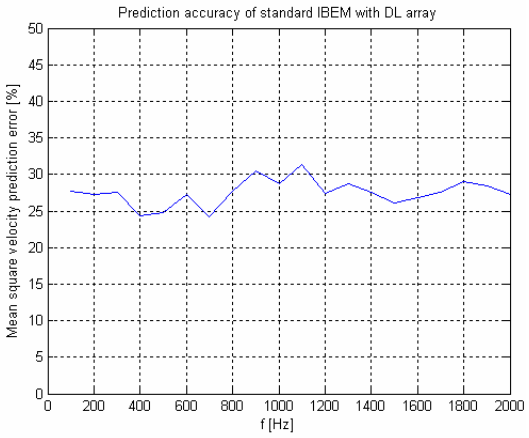

Fig.8 Mean square velocity prediction error with IBEM algorithm with reflections from behind of the array

4.2 Computational cost

Test of computational cost of all NAH algorithms were performed on Centrino based computer station with Pentium M 1.7GHz processor with 1 GB of internal RAM. All algorithms were implemented in MathWorks Matlab v.6.5 R13 and calculation of pressure prediction was performed while calculation time has been measured. The results are only for kernels of the algorithms, no data pre-processing and visualization was taken in account. The Table 1 shows the calculation time for different algorithms with free field conditions (no reflections) and with two setting of kernel parameter (number of numer. integration points, iterations, elements). All results (time and velocity error) are related to prediction of one principal component at 1 kHz.

Algorithm	**Settings**	**Prediction at 1 kHz**	
		Time [s]	Error [%]
DL-SONAH	64 p.int.	0,49	15,5
DL-SONAH	128 p.int.	0,93	14,3
ST-NAH	50 iter.	1,89	40,2
ST-NAH	500 iter.	2,69	23,4
IBEM	2700 ele.	51,4	19,4

Table 1 Computational cost of the algorithms

5 Conclusion

As can be seen from of presented velocity prediction accuracy in near field, inverse BEM algorithm has better reconstruction accuracy than DL-SONAH and ST-NAH, when reflections from behind are present. The reconstruction accuracy of the algorithms for free-field conditions is around 25 percent in the frequency region of interest. The computational cost of the algorithms depends on its complexity, thus IBEM consumes more computational time (more than 50 times with 2700 boundary elements). The comparison of the selected methods confirms shorter calculation time in non-element based methods, especially in DL-SONAH. The calculation time of ST-NAH algorithm with aperture enlargement consume more time due to iterative procedure.

Acknowledgments

The authors would like to thank to Jørgen Hald, Brüel&Kjær, for help with implementation of the Double layer SONAH algorithm and many suggestions during preparation of simulation test cases. This research activity was partially supported by Czech Science Foundation within the project nr. 102/06/1617.

References

[1] J. Hald, "Patch near-field acoustical holography using a new statistically optimal method", *Proceedings of Inter-Noise 2003*, Jeju Island, Korea, 2203-2210 (2003).

[2] J. Hald, "Patch holography in cabin environments using a two-layer handheld array with an extended SONAH algorithm", *Proceedings of Euronoise 2006*, Tampere, Finalnd, (2006).

[3] J. S. Gomes, "*Double layer microphone array*" [Master thesis], Department of Physics, University of Southern Denmark (2005).

[4] Z. Havránek, F. Jacobsen, "Near field acoustic holography with double layer array processing", *Proceedings of Euronoise 2006*, Tampere, Finland, 13-19 (2006).

[5] Y. Fei, C. Jian, B. Chuanxing, L. Weibing and C. Xinzhao, "Experimental investigation of sound field separation technique with double holographic plane", *Chinese Journal of Acoustics* 24, 111-118 (2005).

[6] K. Saijyou, S. Yoshikawa, "Reduction methods of the reconstruction error for large-scale implementation of the near-field acoustical holography", *J. Acoust. Soc. Am.* 110, 2007-2023 (2001).

[7] M. R. Bai, "Acoustical source characterization by using recursive Wiener filtering", *J. Acoust. Soc. Am.* 97, 2657-2663 (1995).

[8] Z. Havránek, S. Klusacek, "Identification of regularization parameter for NAH by comparison of results of different NAH calculation methods", *Proceedings of Inter-noise 2007*, Turkey, 1-9 (2007).

[9] J. S. Gomes, "Comparing Parameter Choice Methods for the Regularization in the SONAH Algorithm", *Proceedings of Euronoise 2006*, Tampere, Finalnd, 7-13 (2006).

[10] Bong-Ki Kim, Jeong-Guon Iha, "On the reconstruction of the vibro-acoustic field over the surface enclosing an interior space using the boundary element method", *J. Acoust. Soc. Am.* 100, 3003-3016 (1996).